ARTICLE NO. 80-4065

J80-155

Dynamics of Submerged Cylindrical Shells with Eccentric Stiffening

50012
80006

Kerry Kier-Ten Chu,* Michael Pappas,† and Harry Herman‡
New Jersey Institute of Technology, Newark, N.J.

A theoretical analysis is presented for treating the free vibrations of submerged, ring-stiffened cylindrical shells with simply supported ends. The effects of the eccentric stiffeners are averaged over the thin-walled isotropic cylindrical shell. The energy method is utilized and the frequency equation is derived from Hamilton's principle. All three degrees-of-freedom are considered. Numerical results are presented for the frequencies of several example shells. Comparisons with previous theoretical and experimental results indicate reasonably good agreement for shells immersed in water, but poorer agreement in vacuum. The inaccuracies are due to limitations of the Donnell type orthotropic shell theory used. The procedure appears well adapted to preliminary optimization studies of shells immersed in water under minimum natural frequency constraints and for optimal separation of the lower frequencies.

Nomenclature

A	= Fourier coefficient
A_r	= cross-sectional area of stiffener
$[A]$	= frequency determinant
A_{ij}	= elements of frequency determinant
$\{B\}$	= amplitude vector
c	= acoustic velocity in the fluid
D	= flexural stiffness of isotropic cylinder wall, $Et^3/[12(1-\mu^2)]$
E	= Young's modulus
F_i	= defined by Eq. (34)
G	= shear modulus
$H_n^{(2)}(KR)$	= Hankel function of the second kind, of order n and argument KR
h	= thickness of cylinder
h_i	= stiffener dimension as shown in Fig. 1
I	= moment of inertia of stiffener about its centroid
J	= torsional constant for stiffener
$K_n(\bar{K}R)$	= modified Bessel function of the second kind, or order n and argument $\bar{K}R$
$K,\bar{K}$	= coefficient of the equation for potential fluid flow
L	= length of cylindrical shell
l	= ring spacing (see Fig. 2)
$\bar{M}$	= mass per unit area
m	= number of longitudinal half-waves
$\bar{N}_x$	= externally applied load resultant in x direction
$\bar{N}_y$	= circumferential stress resultant due to applied pressure
n	= number of circumferential waves
P	= total pressure
P_h	= hydrostatic pressure
P_r	= radiated pressure
$\bar{P}_r$	= amplitude of radial pressure
R	= radius to middle surface of isotropic cylinder
T	= kinetic energy
t	= time variable
V	= potential energy
u,v,w	= displacements in x,y, and z directions, respectively (axial, tangential, and radial)
x,y,z	= orthogonal coordinates defined in Fig. 1 (x and y lie in middle surface of cylinder or plate)
$\bar{U},\bar{V},\bar{W}$	= amplitudes of displacement
$\bar{z}$	= distance from middle surface of cylinder to centroid of stiffener
$\epsilon_{xT},\epsilon_{yT},\gamma_{xyT}$	= normal strains and shearing strain
Λ_i	= defined by Eq. (35)
μ	= Poisson's ratio
ρ	= circular frequency
ϕ	= velocity potential function
Φ	= amplitude of the velocity potential

Subscripts

c	= cylinder
i,j	= integer
r	= stiffening in y direction
w	= water

A comma indicates partial differentiation with respect to the subscript following the comma.

Introduction

SINCE the early efforts of Rayleigh[1] and Love,[2] the vibration of shells in a vacuum has been extensively analyzed. Typical of recent work on prestressed, eccentrically stiffened, cylindrical shells of finite length are the investigations by McElman et al.,[3] using the orthotropic or smeared stiffener approach and Harari and Baron,[4] who consider discrete stiffeners.

The dynamic interaction between shells and fluids has also received considerable attention. Junger[5-7] was the first to analyze the free and forced vibrations of a cylindrical shell submerged in an acoustic medium. He treated an infinitely long, cylindrical shell utilizing plane strain analysis. The transient response of a submerged, infinitely long, right-stiffened cylindrical shell has been studied by Herman and Klosner[8] and Lyons et al.[9] A submerged cylindrical shell of infinite length, having radial surface motion over a stiffened, finite section has been studied by Paslay et al.[10]

Received April 26, 1979; revision received Sept. 14, 1979.

Index categories: Structural Dynamics; Marine Vessel Vibrations.

*Graduate student, Dept. of Mechanical Engineering (deceased).

†Associate Professor, Dept. of Mechanical Engineering. Member AIAA.

‡Professor, Dept. of Mechanical Engineering.

Recently, some interest has been directed toward optimization of submerged shells with eccentric ring stiffeners under natural frequency constraints and/or with dynamic merit criteria.[11-13] Unfortunately, this early work utilizes an in vacuo vibration model yielding excessively large frequency values for the example shells studied which are immersed in water.

The objective of this paper is to develop a more accurate model for such optimal design studies. Donnell-type orthotropic theory along the lines of Refs. 3 is used in this study because of its computational simplicity. Conservation of computational effort is quite important for preliminary optimization investigations, since one often performs parametric optimal design studies so as to determine the characteristics of optimal designs and since optimization for a single set of design parameters often requires several hundred to several thousand sets of frequency determinations. Thus, it is desirable to use the simplest model capable of generating reasonable results.

Governing Field Equations

The well-known field equation for a homogeneous acoustic fluid medium[14] in terms of the notation used herein is

$$\frac{\partial^2\phi}{\partial r^2}+\frac{1}{r}\frac{\partial\phi}{\partial r}+\frac{1}{r^2}\frac{\partial^2\phi}{\partial(y/R)^2}+\frac{\partial^2\phi}{\partial x^2}=\frac{1}{c^2}\frac{\partial^2\phi}{\partial t^2} \tag{1}$$

in which ϕ is the velocity potential function, c the velocity of sound in the fluid, t the time variable, x the shell coordinate parallel to the axis of the structure (Fig. 1), r the variable describing the distance from the shell surface into the fluid, and y the circumferential coordinate at the mean shell radius R.

The velocity potential ϕ and the radiated pressure P_r can be written as

$$\phi=e^{i\omega t}\Phi\cos(ny/R)\sin(m\pi x/L) \tag{2}$$

$$P_r=e^{i\omega t}\bar{P}_r\cos(ny/R)\sin(m\pi x/L) \tag{3}$$

in which Φ is the amplitude of the velocity potential, $\bar{P}_r$ the amplitude of the radiated pressure, ω the circular frequency, m the number of axial half waves, R the mean radius of the cylindrical shell, and L the length of the cylindrical shell.

Substituting Eq. (2) into the governing field equation (1) for the fluid medium yields:

$$\frac{\partial^2\Phi}{\partial r^2}+\frac{1}{r}\frac{\partial\Phi}{\partial r}+\left(\frac{\omega^2}{c^2}-\frac{n^2}{r^2}-\frac{m^2\pi^2}{L^2}\right)\Phi=0 \tag{4}$$

Now let

$$K^2=(\omega/c)^2-(m\pi/L)^2 \tag{5}$$

If the fluid is assumed to be of infinite extent, the solution of Eq. (4) for an outgoing wave is given by

$$\Phi=AH_n^{(2)}(Kr) \tag{6}$$

in which $H_n^{(2)}$ is the Hankel function of the second kind of order n, $H_n^{(2)}=J_n-iY_n$.

The constant A is evaluated by insuring that the velocity of the shell and the velocity of the fluid medium are equal at the shell-fluid interface, $r=R$, i.e.,

$$\frac{\partial w}{\partial t}=\frac{\partial\phi}{\partial r} \tag{7}$$

For a shell simply supported at each end, the radial deflection is assumed to be

$$w=\bar{W}e^{i\omega t}\sin(m\pi x/L)\cos(ny/R) \tag{8}$$

in which $\bar{W}$ = the amplitude of the radial deflection.

Substituting Eqs. (2) and (8) into Eq. (7) results in

$$i\omega\bar{W}=\frac{\partial\Phi}{\partial r} \tag{9}$$

Upon substituting Eq. (6) into Eq. (9), the constant A can be written as

$$A=i\omega\bar{W}/KH_n'^{(2)}(KR) \tag{10}$$

where ( )′ denotes the differentiation with respect to the argument, and $H_n'^{(2)}$ may be obtained from the relation

$$H_n'^{(2)}=\tfrac{1}{2}(H_{n-1}^{(2)}-H_{n+1}^{(2)}) \tag{11}$$

The radiated pressure P_r is related to the velocity potential of the fluid medium by

$$P_r=\rho_w\frac{\partial\phi}{\partial t} \tag{12}$$

in which ρ_w is the density of the fluid. Then

$$P_r=\rho_w\omega^2e^{i\omega t}f(\omega)\,\bar{W}\sin(m\pi x/L)\cos(ny/R) \tag{13}$$

from which

$$\bar{P}_r=\rho_w\omega^2\bar{W}f(\omega) \tag{14}$$

in which

$$f(\omega)=-\frac{2H_n^{(2)}(KR)}{K\{H_{n-1}^{(2)}(KR)-H_{n+1}^{(2)}(KR)\}} \tag{15}$$

When $(\omega/c)^2-(m\pi/L)^2$ is negative, let

$$K=i\bar{K}=i\{(m\pi/L)^2-(\omega/c)^2\}^{1/2} \tag{16}$$

The function $f(\omega)$ can be written in terms of the Bessel function of the second kind of imaginary argument K_n by

$$f(\omega)=K_n(\bar{K}R)/\bar{K}K_n'(\bar{K}R) \tag{17}$$

where

$$K_n(\alpha)=(\pi/2)(-i)^{n+1}H_n^{(2)}(-i\alpha) \tag{18}$$

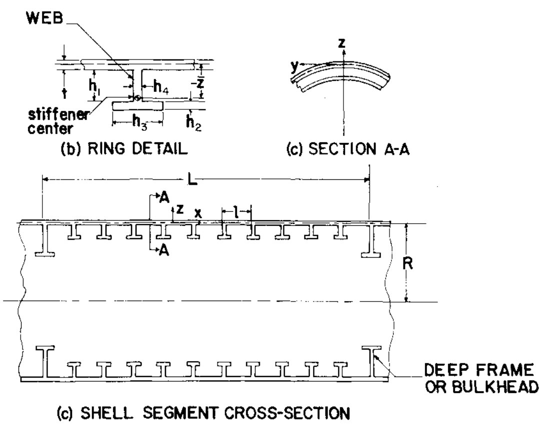

Fig. 1 Shell geometry.

and

$$K_n' = -\tfrac{1}{2}[K_{n-1} + K_{n+1}] \tag{19}$$

Energy of the Stiffened Structure

Consider an axisymmetric structure consisting of a cylindrical shell with reinforcing ring stiffeners. In the cylindrical portion of the structure, the displacements of the shell are defined by the three orthogonal components u,v,w in the x,y,z directions, respectively, which are functions of the coordinates x and y only at the middle surface (see Fig. 1).

The strain energy of the unstiffened thin-walled isotropic cylinder[15] is

$$V_c = \frac{E}{2(1-\mu^2)} \int_{-h/2}^{h/2} \int_0^{2\pi R} \int_0^L (\epsilon_{xT}^2 + \epsilon_{yT}^2 + 2\mu\epsilon_{xT}\epsilon_{yT} + \frac{1-\mu}{2}\gamma_{xyT}^2)\,\mathrm{d}x\mathrm{d}y\mathrm{d}z \tag{20}$$

in which ϵ_{xT}, ϵ_{yT}, and γ_{xyT} are the total normal and shearing strains, E is Young's modulus, and μ is Poisson's ratio. A cylinder may be considered thin walled when the thickness h is sufficiently small compared to the radius R. Usually, $R/h > 60$.

If the displacement in the cylinder and stiffening rings are continuous and the properties of the stiffening rings are averaged over the spacing l, the total strain energy[12] for the stiffening rings of spacing l attached to the shell is found to be

$$V_r = \frac{1}{l}\int_0^{2\pi R} \left(\frac{E_r}{2}\int_0^L \int_{A_r} \epsilon_{xT}^2 \mathrm{d}A_r \mathrm{d}x + \frac{G_r J_r}{2}\int_0^L w,_{xy}^2 \mathrm{d}x\right)\mathrm{d}y \tag{21}$$

The quantity $\mathrm{d}A_r$ is the differential area of the cross-section of the stiffening ring, and $G_r J_r$ is the twisting stiffness of the ring section.

The potential energy of external pressure and an externally applied axial load resultant $\bar{N}_x$ due to the pressure (positive in compression) is

$$V_P = \int_0^{2\pi R}\int_0^L P w \mathrm{d}x\mathrm{d}y + \int_0^{2\pi R} [\bar{N}_x u_T \,|z=\bar{e}]\Big|_0^L \mathrm{d}y \tag{22}$$

where $\bar{N}_x$ is function of P_h in this case; $P = P_h + P_r$; P_h is a constant external pressure; and P_r is radiated pressure. The quantity $\bar{e}$ is the distance from the middle surface of the isotropic shell to the line on which the load resultant $\bar{N}_x$ acts.

The potential strain energy of the combined structure can be written as the sum of the energies of the cylindrical shell, the stiffening rings, and the loads as follows:

$$V = V_c + V_r + V_P \tag{23}$$

The kinetic energy of the system can be written in terms of the kinetic energies of the cylindrical shell segments and the stiffening rings.

If the mass of the ring is smeared over the cylinder the total kinetic energy of the system is given by

$$T = \frac{1}{2}\int_0^L \int_0^{2\pi R} \bar{M}(\dot{u}^2 + \dot{v}^2 + \dot{w}^2)\,\mathrm{d}x\mathrm{d}y \tag{24}$$

where

$$\bar{M} = \rho_c h + \rho_r (A_r/l) \tag{25}$$

is the average or distributed mass per unit area. Here ρ_c and ρ_r are the density of the shell and ring material, respectively, A_r is the ring cross-sectional area, and l is the ring spacing.

Now using the Donnell type nonlinear strain displacement relations,

$$\epsilon_{xT} = u_{T,x} + \tfrac{1}{2} w,_x^2$$
$$\epsilon_{xT} = v_{T,y} + w/R + \tfrac{1}{2} w,_y^2$$
$$\gamma_{xyT} = u_{T,y} + v_{T,x} + w,_x w,_y \tag{26}$$

where

$$u_T = u - z w,_x, \quad v_T = v - z w,_y \tag{27}$$

Now integrating and applying Hamilton's principle,[16] one derives the equations of motion. The deformations associated with the vibration of a prestressed cylinder consist of the axisymmetric static prestress deformations u_A, v_A, and w_A which occur prior to excitation plus the small additional deformations u_B, v_B, and w_B resulting from the excitation. Invoking the boundary conditions, assuming a constant prestress, and ignoring the nonlinear terms associated with the small additional deformations, the expressions for these deformations which satisfy the boundary conditions take the form

$$u_B = \bar{U}e^{i\omega t}\cos(m\pi x/L)\cos(ny/R)$$
$$v_B = \bar{V}e^{i\omega t}\sin(m\pi x/L)\sin(ny/R)$$
$$w_B = \bar{W}e^{i\omega t}\sin(m\pi x/L)\cos(ny/R) \tag{28}$$

where m is the number of axial half-waves and n is the number of circumferential full waves, one obtains

$$-\left(\bar{M}\omega^2 + \frac{Eh}{1-\mu^2}\frac{m^2\pi^2}{L} + Gh\frac{n^2}{R^2}\right)\bar{U} + \frac{mn\pi}{LR}\left(\frac{\mu Eh}{1-\mu^2} + Gh\right)\bar{V} - \frac{\mu Eh}{1-\mu^2}\frac{m\pi}{LR}\bar{W} = 0$$

$$\frac{mn\pi}{LR}\left(\frac{\mu Eh}{1-\mu^2} + Gh\right)\bar{U} - \left(\bar{M}\omega^2 + \frac{Eh}{1-\mu^2}\frac{n^2}{R^2} + \frac{E_r A_r}{l}\frac{n^2}{R^2} + Gh\frac{m^2\pi^2}{L^2}\right)\bar{V} - \frac{n}{R^2}\left(\frac{Eh}{1-\mu^2} + \frac{E_r A_r}{l} + \frac{E_r A_r \bar{z}_r n^2}{lR}\right)\bar{W} = 0 \tag{29}$$

$$\frac{\mu Eh}{1-\mu^2}\frac{\mu m\pi}{RL}\bar{U} - \frac{n}{R^2}\left(\frac{Eh}{1-\mu^2} + \frac{E_r A_r}{l} + \frac{E_r A_r \bar{z}_r n}{lR}\right)\bar{V} - \Bigg\{D\left[\left(\frac{m\pi}{L}\right)^4 + \left(\frac{n}{R}\right)^4 + 2\mu\left(\frac{mn}{LR}\right)^2\right] + \left(\frac{Gh^3}{3} + \frac{G_r J_r}{l}\right)\left(\frac{mn\pi}{LR}\right)^2 + \frac{E_r I_r}{l}\left(\frac{n}{R}\right)^4 + \frac{E_r A_r}{lR^2}\left[1 + \bar{z}_r\left(\frac{2n^2}{R} + \bar{z}_r\frac{n^4}{R^2}\right)\right] + \frac{Eh}{1-\mu^2}\frac{1}{R^2} - \bar{N}_x\left(\frac{m\pi}{L}\right)^2 - \bar{N}_y\left(\frac{n}{R}\right)^2 - [\bar{M} + \rho_w f(\omega)]\omega^2 \bar{W}\Bigg\} = 0$$

Here $\bar{z}_r$ is the distance from the middle surface of the isotropic shell to the centroid of ring cross-section where $\bar{z}_r$ is positive for a stiffening ring on the outer surface of the shell and negative for a ring on the inner surface, and $\bar{N}_y$ is the circumferential line load due to the applied pressure.

The last of these equations contains a term involving $f(\omega)$ which may be real or complex, depending upon whether the K^2 of Eq. (5) is negative or positive, respectively. When $f(\omega)$ is complex, the real part may be considered as the "added mass" effect of the fluid and the imaginary part a form of damping associated with energy loss to the fluid. For the range of frequencies of interest here for shells immersed in water, K^2 will usually be negative, and thus $f(\omega)$ is real. Thus, for the purpose of this study, a frequency equation where $f(\omega)$ is real is developed.

Equation (29) may conveniently be written as

$$[A]\{B\}=0 \tag{30}$$

where

$$\{B\}=\begin{Bmatrix}\bar{U}\\ \bar{V}\\ \bar{W}\end{Bmatrix} \tag{31}$$

This is not, however, a linear eigenvalue problem, since ω occurs in $f(\omega)$.

For the case where $f(\omega)$ is real, the determinant of the displacement coefficients, when set equal to zero, yields the equation for the circular frequency where

$$\Lambda_3\omega^6+\Lambda_2\omega^4+\Lambda_1\omega^2+\Lambda_0=0 \tag{32}$$

$$\Lambda_3=F_1\bar{M}^2$$

$$\Lambda_2=M[F_1(F_2+F_3)-\bar{M}F_7]$$

$$\Lambda_1=F_1[F_2F_3-(F_4)^2]-\bar{M}[(F_2+F_3)F_7-(F_5)^2-(F_6)^2]$$

$$\Lambda_0=[(F_4)^2-F_2F_3]F_7+(F_5)^2F_2+(F_6)^2F_3+2F_4F_5F_6 \tag{33}$$

and

$$F_1=[\bar{M}+\rho_w f(\omega)]$$

$$F_2=\frac{Eh}{1-\mu^2}\frac{m^2\pi^2}{L^2}+Gh\frac{n^2}{R^2}$$

$$F_3=\left(\frac{Eh}{1-\mu^2}+\frac{E_rA_r}{l}\right)\frac{n^2}{R^2}+Gh\frac{m^2\pi^2}{L^2}$$

$$F_4=A_{12}=\left(Gh+\mu\frac{Eh}{1-\mu^2}\right)\frac{mn\pi}{LR}$$

$$F_5=A_{23}=-\left[\frac{Eh}{1-\mu^2}+\frac{E_rR_r}{l}\left(1+\bar{z}_r\frac{n^2}{R}\right)\right]\frac{n}{R^2}$$

$$F_6=A_{13}=\frac{\mu Eh}{1-\mu^2}\frac{m\pi}{LR}$$

$$F_7=D\left[\left(\frac{m\pi}{L}\right)^4+\left(\frac{n}{R}\right)^4+2\mu\left(\frac{mn\pi}{LR}\right)^2\right]$$
$$+\left(\frac{Gh^3}{3}+\frac{G_rJ_r}{l}\right)\left(\frac{mn}{LR}\right)^2+\frac{E_rI_r}{l}\left(\frac{n}{R}\right)^4$$
$$+\frac{E_rA_r}{lR^2}\left[1+\bar{z}_r\left(\frac{2n^2}{R}+\bar{z}_r\frac{n^4}{R^2}\right)\right]$$
$$+\frac{Eh}{1-\mu^2}\frac{1}{R^2}-\bar{N}_x\left(\frac{m\pi}{L}\right)^2-\bar{N}_y\left(\frac{n}{R}\right)^2 \tag{34}$$

After the natural frequency ω is obtained by equating the determinant $[A]$ to zero and substitution of the value of ω into Eq. (30), the nontrivial solution will provide the amplitude ratios from the three algebraic equations of the coefficients of $\bar{U}$, $\bar{V}$, and $\bar{W}$.

Where only one-degree-of-freedom is to be considered, only the radial surface motion of the system is permitted and other surface motions are neglected. The frequency equation is derived from det $[A]=0$ by equating $\bar{M}\omega^2$ terms to zero in the first two diagonal elements of $[A]$. This equation has the following

$$\Lambda_1'\omega_0^2+\Lambda'=0 \tag{35}$$

Numerical Procedures

Both the three- and one-degree-of-freedom frequency equations, Eqs. (32) and (35), respectively, must be solved numerically since some coefficients are functions of ω. For this paper, a sequence of values of ω were substituted into the left-hand side of Eq. (32) and a bisection method employing the secant rule[17] used to locate a root when a change in the sign of the left-hand side occurred. This technique was used to investigate the possibility of multiple real roots. None were found. A similar procedure was used for the single degree of freedom equation for programming convenience.

Such procedures are, of course, too computationally wasteful for optimization work. In the optimal design situation, one almost always has a very close, or may obtain a reasonably close, estimate of the value ω satisfying Eq. (32) or (35). Thus, one may effectively use successive substitutions to solve these equations in relatively few iterations. For example, Eq. (32) may be treated as an eigenvalue problem, where the $f(\omega)$ term is computed using the close approximation, to obtain a still closer approximation. This procedure would be repeated until convergence occurred. Equation (35) could be solved similarly. Thus, although the computational effort associated with frequency determination of submerged structures would be several times greater than those in vacuo, the amount of effort would still be low enough for preliminary optimization studies, since the in vacuo studies were not particularly computationally demanding,[12] particularly if the one-degree-of-freedom equation yields satisfactory accuracy.

Results and Comparisons

Five example shells were analyzed in vacuum and in water so as to examine the effect of immersion in water, to examine the accuracy of the formulation described herein, and to compare the accuracy of the Donnell- and Flügge-type shell theories. In addition, for several examples the effect of stiffener eccentricity was examined.

The first group consists of three shells developed in the studies of Ref. 11 and design examples using a minimum frequency constraint from Ref. 12 immersed in sea water at a depth of 304.8 m (1000 ft). They will be referred to as examples 1, 2, and 3, respectively. These shells are analyzed in water and in vacuo, where for the latter the effects of the hydrostatic pressure of immersion are considered. Shells with outside stiffeners are also analyzed in addition to the inside stiffened configurations of Refs. 11 and 12. The parameters used for these studies are: $R=5.029$ m (198 in.), $L=15.088$ m (594 in.), $\mu=0.33$, $E=2.068\times10^5$ MPa (30×10^6 psi), $\rho_c=7.830\times10^{-3}$ g/mm^3 (7.33×10^{-4} slug/in.^{3}), $\rho_w=1.035\times10^{-3}$ g/mm^3 (0.969×10^{-4} slug/in.^{3}), $c=1524$ m/s (60,000 in./s), depth of immersion 304.8 m (1000 ft).

For example 1:

$h=30.622$ mm (1.2056 in.), $l=766.32$ mm (30.17 in.), $h_1=279.91$ mm (11.02 in.), $h_2=7.800$ mm (0.3071 in.), $h_3=263.22$ mm (10.363 in.), $h_4=6.027$ mm (0.2373 in.).

For example 2:

$h=31.029$ mm (1.2216 in.), $l=859.79$ mm (33.85 in.), $h_1=526.29$ mm (20.72 in.), $h_2=11.819$ mm (0.4653 in.), $h_3=445.77$ mm (17.55 in.), $h_4=10.033$ mm (0.3950 in.).

For example 3:
$h=29.522$ mm (1.1623 in.), $l=424.43$ mm (16.71 in.), $h_l=239.04$ mm (9.411 in.), $h_2=4.653$ mm (0.1832 in.), $h_3=150.80$ mm (5.937 in.), $h_4=5.105$ mm (0.2010 in.).

These shells differ primarily in the nature of their stiffeners. Example 2 employs relatively large, widely spaced stiffeners, while example 3 uses relatively small, closely spaced stiffeners.

The effect of immersion in water, of ignoring the u and v motion components, and stiffener eccentricity are very similar for all these examples. Thus, only the results of example 1 are presented in tabular form. It may be seen from Table 1 and Fig. 2 that the natural frequency behavior of the in vacuo model for shells immersed in water is grossly inaccurate, particularly with respect to frequency separation which is much less in water. Thus, the in vacuo model does not seem appropriate for optimal frequency separation studies.

Other differences are also apparent. Although there is a substantial difference between frequencies computed using three-degrees-of-freedom [Eq. (32)] and one-degree-of-freedom [Eq. (35)] with the in vacuo model, particularly where $n=1$, this difference is for practical purposes negligible for shells considering the fluid interaction effects of water. The largest difference for shells immersed in water also occurred at $n=1$. However, here the difference was typically only about 3%. Thus, only one-degree-of-freedom need be considered for such shells.

Comparing Tables 1 and 2, it may be seen that stiffener eccentricity has little effect except at the lower frequencies where outside stiffeners produced lower values. Thus, for optimization under a minimum frequency constraint, inside stiffeners seem more effective.

A comparison of Donnell vs Flügge theory for examples 1 and 2 is given in Table 3. It may be seen that Donnell theory yields substantially higher values for the lower in vacuo frequencies. As will be seen from example 5, this difference represents a greater inaccuracy on the part of the Donnell theory at these frequencies.

Example 4 is used to provide some correlation between the present analysis and experimental results[10] for shells immersed in water. Unfortunately, the differences in end conditions cloud the comparison somewhat. Still, this comparison is useful since for such shells the effect of end conditions is not great. A comparison with experiments in air is also provided. For this example:

$R=0.5144$ m (20.25 in.), $L=1.289$ m(60.75 in.), $\mu=0.3$, $E=2.068\times10^5$ MPa (30×10^6 psi), $\rho_c=8.300\times10^{-3}$ g/mm^3

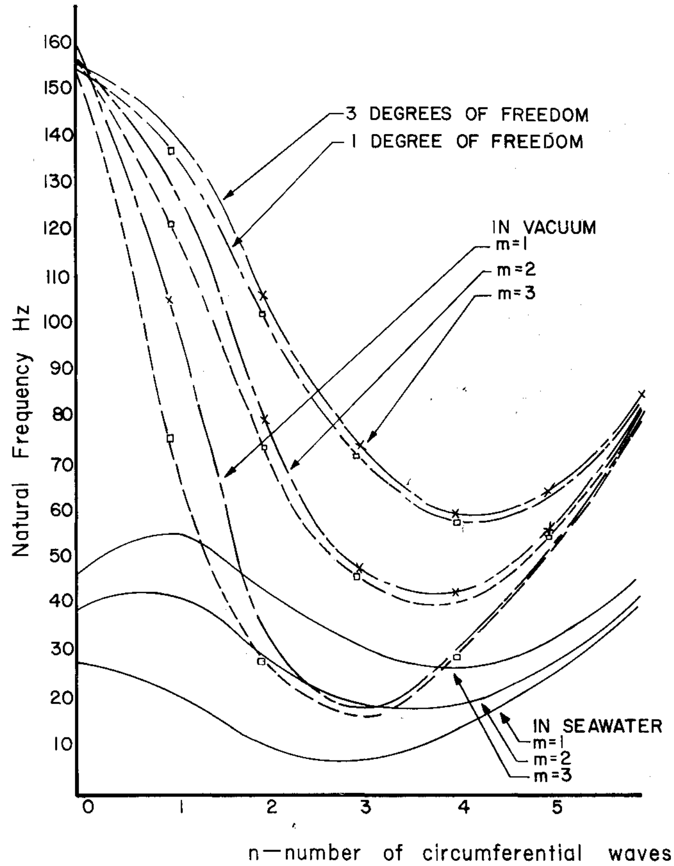

Fig. 2 Natural frequencies for example 1 shell.

(7.77×10^{-4} slug/in.^{3}), $\rho_w=0.9977\times10^{-3}$ g/mm^3 (0.934×10^{-4} slug/in.^{3}), $c=1524$ m/s (60,000 in./s), depth of immersion $=1.524$ m (5 ft), $h=4.496$ mm (0.177 in.), $l=85.72$ mm (3.375 in.), $h_l=45.29$ mm (1.783 in.), $h_2=0$, $h_3=0$, $h_4=4.597$ mm (0.181 in.).

It may be seen from Table 4 that the one-degree-of-freedom model used here provides reasonable agreement with experiment. Considering three-degrees-of-freedom produces slightly poorer results due to the inaccuracy inherent in the Donnell theory for shells of such parameters. Agreement is better for shells in water than in air. This is, of course, ex-

Table 1 Natural frequencies, Hz, example 1—inside frames

n \ m	1		2		3	
	Degrees of freedom					
	3	1	3	1	3	1
In sea water						
0	29.4	29.4	39.5	39.5	46.8	46.8
1	23.0	22.4	43.9	43.5	56.7	56.5
2	10.3	10.2	29.3	28.9	44.6	44.4
3	6.96	6.90	19.8	19.6	33.4	33.2
4	13.14	13.08	18.8	18.7	28.1	28.0
5	24.8	24.7	27.2	27.1	32.1	32.0
6	40.4	40.3	41.9	41.8	44.6	44.5
In vacuum						
0	162	158	159	158	158	157
1	107	76.8	133	123	142	139
2	34.3	29.5	81.7	74.9	108	104
3	18.6	17.6	49.1	46.6	76.1	73.4
4	30.8	30.0	42.4	41.2	60.0	58.6
5	53.1	52.2	56.8	55.9	64.5	63.6
6	80.8	80.0	82.2	81.4	85.2	84.4

Table 2 Natural frequencies, Hz, example 1—outside frames

$n \setminus m$	1		2		3	
	Degrees of freedom					
	3	1	3	1	3	1
In sea water						
0	29.4	29.4	39.5	39.5	46.8	46.8
1	23.2	22.5	44.3	43.1	57.4	57.1
2	10.2	10.0	30.3	28.8	46.4	46.0
3	5.85	5.79	20.5	20.3	36.0	35.7
4	12.1	12.1	18.4	18.3	30.3	30.1
5	24.2	24.0	26.2	26.0	32.8	32.6
6	40.0	39.8	40.8	40.6	44.2	43.9
In vacuum						
0	162	158	159	158	158	157
1	109	77.4	134	125	144	141
2	34.5	29.2	85.3	77.4	113	108
3	15.8	14.2	51.5	48.2	82.7	79.1
4	29.0	27.8	42.0	40.2	65.3	62.9
5	52.3	50.8	55.2	53.6	66.7	64.8
6	80.7	79.0	80.9	79.1	85.3	83.4

Table 3 Comparison of frequencies with method of Ref. 11, Hz

	Example 1			Example 2		
	Ref. 11[a]	Chu[b]	Chu[c]	Ref. 11[a]	Chu[b]	Chu[c]
ω_1	12.03	17.6	18.62	28.37	36.70	41.50
ω_2	22.90	29.52	30.81	51.96	58.58	60.88
ω_3	30.30	30.00	34.27	51.96	68.17	70.55

[a] Flügge theory, three-degrees-of-freedom. [b] Present analysis—Donnell theory, one-degree-of-freedom. [c] Present analysis—Donnell theory, three-degrees-of-freedom.

Table 4 Comparison of natural frequencies with Pasley et al.[10], Hz

$n \setminus m$	1		2	
	Pasley[10]	Chu[a]	Pasley[10]	Chu[a]
In water				
2	128/134	147	414	509
3	204	218	382	428
4	373	395	466	512
5	599	657	655	733
6	860	999	902	1046
In air				
2	262/270	322	—	921
3	369/383	424	—	738
4	650	719	760	809
5	990	1127	1036	1089

[a] Present one-degree-of-freedom analysis.

pected since the inaccuracies in the Donnell theory affect only the shell stiffener terms and thus this improvement in accuracy in water indicates that the fluid structure interaction model yields good results.

The final example is used to provide a more extended comparison between Donnell and Flügge theories. The parameters for this study are:

$R=259.1$ mm (10.2 in.), $L=762$ mm (30.0 in.), $\mu=0.33$, $E=6.895\times10^4$ MPa (10×10^6 psi), $\rho_c=2.713\times10^{-3}$ g/mm (2.54×10^{-4} slug/in.^{3}), $\rho_w=1.035$ g/mm^3 (9.69×10^{-5} slug/in.^{3}), $c=1524$ m/s (60,000 in./s), depth of immersion$=0$ m (0 ft), $h=8.382$ mm (0.330 in.), $l=127$ mm (5.00 in.), $h_1=25.4$ mm (1.00 in.), $h_2=h_3=0$, $h_4=9.525$ mm (0.375 in.).

The results for the in vacuo study are compared in Table 5 with those given by Harari and Baron.[4] It may be seen that at the lower frequencies the difference is again quite pronounced, although proportionally less than in examples 1 and 2, where stability effects contribute substantially and thus Donnell inaccuracies are compounded. Divergence between theories increases with increasing m and decreases with increasing n. Unfortunately, at larger n, where agreement between theories is good, orthotropic theory produces poor results.[4]

Thus it appears that, although the present method gives reasonably good results for shells immersed in water, use of the Flügge theory could significantly improve accuracy.

Example 4 was also examined for effects of stiffener eccentricity and ignoring the u and v motions as was example 5, which was also analyzed for frequencies immersed in water. Results produced closely followed those of examples 1-3 with regard to these effects, except that the effect of stiffener placement and use of only 1 deg of freedom were even less significant in examples 4 and 5.

Conclusions

The procedure for calculation of frequencies of submerged shells described here seems quite adequate for preliminary optimization studies of shells immersed in water. The simplicity of the shell model and the fact that only one degree-of-freedom need be considered allows rapid evaluation of

Table 5 Comparison of natural frequencies in vacuum with experiment and Harari and Baron, Hz

n \ m	1			2			3		
	Ref. 18[a]	Ref. 4[b]	Chu[c]	Ref. 18[a]	Ref. 4[b]	Chu[c]	Ref. 18[a]	Ref. 4[b]	Chu[c]
0	—	—	—	—	—	—	3020	3105	3096
1	1232	1133	1526	—	—	—	—	—	—
2	627	640	756	—	—	—	—	—	—
3	787	832	922	1190	1194	1381	1602	1650	1923
4	1310	1432	1483	1503	1575	1764	1806	1826	2183
5	1938	2253	2253	2059	2331	2483	2276	2474	2839
6	2594	3276	3205	—	—	—	2602	3424	3753
7	3179	4466	4334	—	—	—	—	—	—
8	3728	5853	5637	—	—	—	—	—	—

[a] Experimental results. [b] Harari and Baron orthotropic theory. [c] Present one-degree-of-freedom analysis.

frequency behavior, an important asset for optimization, which usually requires several hundred sets of such evaluations for the determination of one optimal design. For all modes of interest here the radiated pressure was real and thus the procedure readily allows consideration of the fluid interaction effect. Thus, the existing method seems well adapted for preliminary optimization under a minimum frequency constraint or for optimal frequency separation problems involving the lower frequencies.

Use of a Flügge-type shell theory would improve accuracy and make the procedure more useful for design purposes. Extension to treat cases where the radiated pressure is complex is straightforward.

The primary limitation of the method given here, even with the above extensions, in treating the optimal frequency separation problem is the possible presence of active inter-ring vibration modes at the optimum.[13] Realistic treatment in such circumstances requires use of discrete theory[4,18] and its associated large computational effort. Even this extension is probably tractable in light of current optimization developments.[19,20] The other important limitation results from the fact that the end effects would play an important role in frequencies associated with primarily axial models, although these fluid effects should be less important here than they are for primarily axial modes. The inclusion of these effects is a formidable problem, particularly if an approach considering these effects is to be used for the purposes of optimization. Thus, the prospects of early development of reasonably accurate optimization procedures for primarily axial frequency separation seems remote.

Acknowledgment

Supported by the Office of Naval Research under Contract No. ONR N00014-75-C0987 and the Foundation at New Jersey Institute of Technology. This work is based in part on the Doctoral dissertation of the first author.

References

[1] Rayleigh, J.W.S., *The Theory of Sound*, Dover Publications, New York, 1945, pp. 395-432.

[2] Love, A.E.H., *Treatise on the Mathematic Theory of Elasticity*, Dover Publications, New York, 1944, pp. 537-552.

[3] McElman, J. A., Mikulas, M. M., Jr., and Stein, M., "Static and Dynamic Effects of Eccentric Stiffening of Plates and Cylindrical Shells," *AIAA Journal*, Vol. 4, May 1966, pp. 887-894.

[4] Harari, A. and Baron, M. L., "Analysis for the Dynamic Response of Stiffened Shells," *Transactions of ASME, Journal of Applied Mechanics*, Vol. 40, Series E, 1973, pp. 1085-1090.

[5] Junger, M. C., "Radiation Loading of Cylindrical and Spherical Surface," *Journal of the Acoustical Society of America*, Vol. 24, May 1952, p. 288.

[6] Junger, M. C., "The Physical Interpretation of the Expression for an Outgoing Wave in Cylindrical Coordinates," *Journal of the Acoustical Society of America*, Vol. 25, Jan. 1953, p. 40.

[7] Junger, M. C., "Vibrations of Elastic Shell in a Fluid Medium and the Associated Radiation of Sound," *Transactions of ASME, Journal of Applied Mechanics*, Vol. 74, 1952, pp. 439-445.

[8] Herman, H. and Klosner, J. M., "Transient Response of a Periodically Supported Cylindrical Shell Immersed in a Fluid Medium," *Transactions of ASME, Journal of Applied Mechanics*, Vol. 32, Series E, 1965, pp. 562-568.

[9] Lyons, W. C., Russell, J. E., and Herrmann, G., "Dynamics of Submerged Reinforced Cylindrical Shell," *Journal of Engineering Mechanics Div., ASCE*, Vol. EM2, April 1968, pp. 397-420.

[10] Paslay, R. B., Tatge, R. B., Wernick, R. J., Walsh, E. K., and Muster, D. F., "Vibration Characteristics of a Submerged Ring-Stiffened Cylindrical Shell of Finite Length," *Journal of the Acoustical Society of America*, Vol. 46, No. 3 (part 2), 1969, pp. 701-710.

[11] Bronowicki, A. J., Nelson, R. B., Felton, L. P., and Schmit, L. A., Jr., "Optimization of Ring Stiffened Cylindrical Shells," *AIAA Journal*, Vol. 13, Oct. 1975, pp. 1319-1324.

[12] Pappas, M., "Improved Synthesis Capability for "T" Ring-Stiffened Cylindrical Shells Under Hydrostatic Pressure," *Computers and Structures*, Vol. 6, 1976, pp. 339-343.

[13] Pappas, M., "Optimal Frequency Separation of Cylindrical Shells," *AIAA Journal*, Vol. 16, Sept. 1978, pp. 999-1001.

[14] Prandtl, L. and Tietjens, O. G., *Fundamentals of Hydro- and Aeromechanics*, Dover Publications, New York, 1957, p. 131.

[15] Timoshenko, S. P. and Gere, J. M., *Theory of Elastic Stability*, McGraw-Hill Book Co., New York, 1964, pp. 265-443.

[16] Langhaar, H. L., *Energy Methods in Applied Mechanics*, John Wiley and Sons, Inc., New York, 1962, pp. 233-239.

[17] Shampine, L. F. and Allen, R. C., Jr., *Numerical Computing*, W. B. Saunders Co., Philadelphia, 1973, pp. 88-100.

[18] Basdekas, N. L. and Chi, M., "Response of Oddly Stiffened Circular Cylindrical Shells," *Journal of Sound and Vibration*, Vol. 17, 1971, pp. 187-206.

[19] Moradi, J. Y. and Pappas, M., "A Boundary Tracking Algorithm for Constrained Nonlinear Problems," *Transactions of ASME, Journal of Mechanical Design*, Vol. 100, pp. 242-266.

[20] Pappas, M. and Moradi, J. Y., "Optimal Design of Ring Stiffened Cylindrical Shells Using Multiple Frame Sizes," New Jersey Institute of Technology Rept. NV-14, July 1978.